A generalized approach to modeling absorption and photocurrent in solar cells with light scattering structures

Joseph Murray[1,2] and Jeremy N. Munday[1,2,a)]
[1]*Department of Electrical and Computer Engineering, University of Maryland, College Park, Maryland 20742, USA*
[2]*Institute for Research in Electronics and Applied Physics, University of Maryland, College Park, Maryland 20740, USA*

(Received 25 July 2016; accepted 9 October 2016; published online 27 October 2016)

The spatial dependence of absorption in optical structures is important for determining the performance of optoelectronic devices, such as solar cells and photodetectors. When random scattering structures are introduced, the absorption can be difficult to calculate without direct simulation or broad simplifying assumptions. Here we present a theoretical framework for calculating the absorption in individual layers of arbitrary stratified media composed of any combination of coherent thin-films and/or incoherent thick slabs in the presence of randomizing scattering structures. This model allows for accurate predictions of generated carriers in photovoltaic systems. We discuss how these equations may be implemented to describe several common special cases as well as a few complex, non-traditional structures to show the wide range of applicability. Finally, we perform experiments on two multilayer structures with interlaced scattering layers to demonstrate utility and accuracy of the technique. *Published by AIP Publishing.*
[http://dx.doi.org/10.1063/1.4965874]

I. INTRODUCTION

Understanding where absorption takes place within an optoelectronic device (e.g., a solar cell or photodetector) is essential to evaluating its performance. Absorption in the active layers leads to carrier generation, while absorption outside of those regions represents energy loss. While the total absorption may be of interest, knowing the location of absorption allows researchers to properly evaluate trade-offs and optimize device efficiency. For simple, non-scattering stratified structures, this calculation is either performed directly by finding the electromagnetic field throughout the individual layers[1,2] or by finding the total absorption and neglecting less absorptive layers. When scattering structures are introduced, these calculations can be more difficult. If these structures contain coherent scatterers such as gratings or periodic arrays of particles, the absorption in each layer can be found by calculating the fields using rigorous coupled-mode theory,[3,4] finite element simulations,[5–8] or, in some cases, analytic expressions.[9,10] However, when scattering occurs from non-periodic (random) configurations, these techniques are no longer applicable. In these cases, calculating absorption in individual layers requires either aggregates of randomized sub-simulations[11] (e.g., Monte Carlo techniques), simplifying assumptions (e.g., no absorption in all other layers), or using analytic expressions for the limit of absorption assuming ideal randomization of the light and/or optimal mode coupling.[7,8,10,12–17] The modeled transmission and reflection from white paint back reflectors on thin-film silicon solar cells has also been considered in Ref. 18; however, such calculations do not provide the absorption in individual layers, which is particularly useful for complex structures in the presence scattering. Thus, there is a need for complete analytic results that can quickly and accurately describe absorption in individual layers of more elaborate structures that incorporate scattering, coherent layers, and incoherent layers.

Here we present analytic expressions for absorption in individual layers of arbitrary stratified planar media (having any combination of thin coherent films and thick incoherent slabs) containing randomizing scattering structures. We focus our discussion on structures with planar scattering layers that completely randomize the light in that layer. The framework is most directly applicable to layers of dielectric scatterers, as we will use the effective refractive index ensemble model,[19] and will be limited to weakly absorbing scattering layers (no such constraints are placed on other layers). However, the equations are completely agnostic toward the nature of the scattering (i.e., how the scattering is achieved) and only require that it can be described by parameters that can be determined experimentally. Note that this method yields fully analytic results, differing from approaches that use analytic expression incorporating simulated scattering.[6–8] We then give examples of how to implement these models in several special cases. We show how this model can be used to describe a variety of interesting structures and compare two examples to experimental measurements.

The methods presented here have several benefits over previously developed techniques. Finite element methods are good for periodic structures but are computationally expensive for randomly distributed scatterers and do not provide the same level of physical insight as analytical solutions. Further, unlike other spectral flux methods, we introduce an effective index model, which only requires three parameters that can be determined experimentally. Our technique

a)Electronic mail: jnmunday@umd.edu

enables us to derive analytic solutions for the absorption in individual layers with arbitrary sets of coherent and incoherent layers, enabling fast computation for complex device architectures.

II. CALCULATING TOTAL ABSORPTION

Total absorption, reflection, and transmission in the absence of scattering can be calculated by Fresnel coefficients using the matrix transfer method with coherent reflection/transmission (at thin-film interfaces) and incoherent reflection/transmission (at interfaces with thick layers such as a glass substrate or a bulk material) following Mitsas and Siapkas.[20] This well-known method calculates the coefficients in two steps. First, field transfer matrices are used to calculate the intensity of reflection/transmission between incoherent layers (or to outside the stack). Second, intensity transfer matrices are used to calculate the total reflection/transmission. Partial coherence may also be introduced by simple modifications to field transfer matrices.[20,21] When a scattering layer is present, the total absorption, reflection, and transmission can similarly be determined depending on the nature of the scattering.[4,7,8,11,18,19,22–24] To account for planar structures with an arbitrary combination of layers, some knowledge of the scattering material is required in order to accurately model the fraction of light that enters or exits the scattering layer. When the light entering the scattering structure becomes completely randomized before returning to one of the two interfaces, only a few parameters are needed to describe the scattering layer (note that randomization does not mean that this layer creates a Lambertian scattering distribution, but that light inside this layer has constant power per solid angle; see below and Ref. 19 for further discussion). We previously showed that in this randomizing regime, the only parameters necessary to accurately describe light propagation in this layer are the experimentally measurable values of internal loss, transmission, and the ensemble of effective indices present at the interfaces of the scattering layer.[19] Here we use the effective index ensemble model because it physically describes many cases of interest, it gives insight into the nature of random scattering, and because its generality allows for modeling of a wide variety of scattering structures. The effective index ensemble model takes the heterogeneous nature of scattering materials into account by assigning a distribution of effective indices to describe the interface with a scattering layer. This ensemble may be approximated by a single index, producing a Lambertian or focused Lambertian scattering distribution, but in general, results in a scattered intensity per solid angle of

$$I(\theta) = I_0 \cos(\theta) \left\langle T(\theta, n_{\text{eff}}, n) P(n_{\text{eff}}) \left(\frac{n}{n_{\text{eff}}}\right)^2 \right\rangle_{n_{\text{eff}}}, \quad (1)$$

where n is the index of refraction for the material into which the scattering occurs, θ is the angle from surface normal inside the material into which the scattering occurs, n_{eff} is an independent variable that is bounded by the minimum and maximum indices of the materials in the scattering layer, $P(n_{\text{eff}})$ is the probability of scattering from a given effective index (note that this function is what defines the ensemble of effective indices, and is in general, a continuous function), $T(\theta, n_{\text{eff}}, n)$ is the transmission coefficient for light exiting the scattering layer, and $\langle\,\rangle_{n_{\text{eff}}}$ indicates the average over the ensemble of indices. Eq. (1) follows directly from our definition of random (constant power at each solid angle). Note that when $Im\{n_{\text{eff}}\}$ is non-negligible, i.e., when the condition $Im\{n_{\text{eff}}\}/Re\{n_{\text{eff}}\} \ll 1$ fails, angles become complex and lose the simple meaning they had in our definition of random and in Eq. (1). In this case, randomization must be understood in the more general sense of equally filling all modes. Our discussion is limited to weakly absorbing scattering layers (other layers are not restricted in this way), which covers most cases of interest. However, Table I and Appendix A show special case, including the addition of absorbing scatterers.

With scattering specified as above, we can calculate the total reflection, transmission, and absorption for the general scattering structure shown in Fig. 1. A scattering layer (s') is sandwiched between an arbitrary set of incoherent layers (denoted by primed letters ranging from a' to b') and coherent layers (unprimed letters from a to b). This structure contains incoherent layers interlaced with arbitrary sets of coherent layers. In general, t and r refer to field transmission and reflection coefficients and T and R refer to intensity coefficients. Subscripts will denote the origin and endpoint layers for light in the calculation of a given coefficient with no propagation beyond the origin and endpoint. For example, $T_{a'b'}$ is be the transmitted intensity for light originating just inside layer a' at the interface nearest layer b' and ending just inside layer b' at the interface nearest layer a'. Note that in the presence of absorbing layers some typical identities for these coefficients no longer apply (e.g., $R_{a'b'} \neq R_{b'a'}$); so, subscript ordering should be carefully noted. Under this scheme, the general scattering distribution described above results in total structure reflection, transmission, and absorption given by

$$R_{a'b'} = \langle R_{a's'} \rangle + \frac{\langle T_{a's'} \rangle \langle T_{\text{diff},s'a'} \rangle \langle R_{\text{scat}} \rangle}{1 - \langle R_{\text{diff},s'a'} \rangle \langle R_{\text{scat}} \rangle}, \quad (2a)$$

$$T_{a'b'} = \frac{\langle T_{a's'} \rangle \langle T_{\text{scat}} \rangle}{1 - \langle R_{\text{diff},s'a'} \rangle \langle R_{\text{scat}} \rangle}, \quad (2b)$$

and

$$A_{a'b'} = 1 - R_{a'b'} - T_{a'b'}, \quad (2c)$$

respectively, where

$$\langle R_{\text{scat}} \rangle = (1 - \tau_{\text{int}}) \rho_{\text{int}} + \frac{(\tau_{\text{int}} \rho_{\text{int}})^2 \langle R_{\text{diff},s'b'} \rangle}{1 - (1 - \tau_{\text{int}}) \rho_{\text{int}} \langle R_{\text{diff},s'b'} \rangle}, \quad (2d)$$

and

$$\langle T_{\text{scat}} \rangle = \frac{\tau_{\text{int}} \rho_{\text{int}} \langle T_{\text{diff},s'b'} \rangle}{1 - (1 - \tau_{\text{int}}) \rho_{\text{int}} \langle R_{\text{diff},s'b'} \rangle}, \quad (2e)$$

and $\langle\ \rangle$ denotes averaging over the effective index ensemble and over both polarizations (note that while we assume the polarization is lost inside the scattering layer, Fresnel coefficients are still polarization dependent). ρ_{int} and τ_{int} are two parameters that characterize the scattering layer and can be determined experimentally. ρ_{int} is the sum of the reflected light and transmitted light intensities ($\rho_{\text{int}} = R + T$), and τ_{int} is the ratio of the transmitted intensity to ρ_{int}, i.e., $\tau_{\text{int}} = \frac{T}{\rho_{\text{int}}} = \frac{T}{R+T}$. Thus $\rho_{\text{int}}\tau_{\text{int}}$ is the fraction of light transmitted from one side of the scatterer to the other and $\rho_{\text{int}}(1-\tau_{\text{int}})$ is the fraction reflected back. $R_{a's'}$ and $T_{a's'}$ are the fractions of direct illumination reflection and transmission, respectively, corresponding to light passing through all layers a' to s'. $R_{\text{diff},s'a'}$ and $T_{\text{diff},s'a'}$ ($R_{\text{diff},s'b'}$ and $T_{\text{diff},s'b'}$) are the total integrated diffuse reflection and transmission for light traveling from the scatterer to outside the front (back) surface. These values can be calculated from the angularly dependent reflection and transmission. For instance, the diffuse reflection for light leaving the scattering layer and travelling out through the front of the structure is given by

$$R_{\text{diff},s'a'} = 2\int_0^{\frac{\pi}{2}} R_{s'a'}(\theta_{s'})\cos(\theta_{s'})\sin(\theta_{s'})d\theta_{s'}. \tag{3a}$$

$\theta_{s'}$ is the angle from the normal in the scattering layer (not the angle of the light escaping the surface). Lastly, direct illumination is not a requirement of the model and diffuse illumination can be implemented by changing $R_{a's'}$ and $T_{a's'}$ in Eqs. (2a) and (2b) to their diffuse counterparts, $R_{\text{diff},a's'}$, and $T_{\text{diff},a's'}$. As an example (in direct analogy to Eq. (3a)), the diffuse reflection resulting from diffuse illumination is

$$R_{\text{diff},a's'} = 2\int_0^{\frac{\pi}{2}} R_{a's'}(\theta_{a'})\cos(\theta_{a'})\sin(\theta_{a'})d\theta_{a'}, \tag{3b}$$

where $\theta_{a'}$ is the incident angle in the front semi-infinite space (Fig. 1).

III. CALCULATING ABSORPTION IN INDIVIDUAL LAYERS

In this section, we demonstrate how to calculate the absorption in individual layers of stratified media containing scattering layers by working through levels of abstraction up to the full scattering structure shown in Fig. 1. We first consider a stack of coherent layers and determine the absorption in individual layers. Second, we consider how this absorption is modified when this stack of coherent layers is part of a larger structure containing both coherent and incoherent layers and determine the absorption in a single incoherent layer for this case. Finally, we use our result to calculate the absorption in each layer (coherent or incoherent) of the full structure (containing coherent, incoherent, and scattering layers) shown in Fig. 1.

Before proceeding to the calculation, some additional discussion on notation is needed. In general, a single subscript denotes the layer corresponding to that parameter (e.g., n_j is the refractive index of the jth layer). Absorption coefficients that use one subscript denote single pass absorption within that incoherent layer (starting just inside the layer on one side to just inside the same layer at the opposite surface). Three subscripts will be used for absorption in multilayers—indicating the layer in which the light originates, the layer in which absorption is calculated, and the endpoint layer, respectively. Furthermore, the propagation direction will be specified by a relative parallel (to the surface) k-vector, $q = \frac{k_\parallel}{k_0}$ where $k_\parallel = nk_0\sin\theta$ (note that this value, q, is constant in all layers in the absence of scattering). If there is no absorption, θ has its usual meaning, the angle from normal in a material of refractive index n. However, within dispersive structures θ is in general complex. Also note that, as done above, we eschew the typical matrix notation and instead opt for explicit equations because the former does not reduce notation or increase clarity due to the large number of unique named variables (see Appendix B for a complete list of variables and constants).

Figure 2 shows a schema of the electric field components propagating forward (+) and backward (−) in a stack of coherent layers, enumerated from a to b. The inset of this figure shows the field components in the jth layer. The absorption in a given coherent layer (defined as the intensity loss in that layer as light travels through the entire coherent stack), for a given propagation direction, is calculated following Pettersson *et al.*[1] and Centurioni.[2] To find the absorption in a given layer, we calculate the energy density in that layer, which is proportional to absorption. Absorption in the jth layer of a single stack of coherent layers due to light originating just outside of the stack (i.e., in the i'^{th} layer) and passing through the entire stack (i.e., to the $(i'+1)^{\text{th}}$ layer) is given by

$$\tilde{A}_{i'j(i'+1)}(q) = \int_0^{d_j} \frac{1}{2}\frac{c\varepsilon_0\alpha_j Re\{n_j\}\left[|E_{\perp,j}(x,q)|^2 + |E_{\parallel,j}(x,q)|^2\right]dx}{Re\left\{\sqrt{1-\left(\frac{q}{n_{i'}}\right)^2}\right\}Re\{n_{i'}\}}, \tag{4a}$$

where the tilde is used to distinguish the absorption in j for a single coherent stack from general case, including incoherent layers, defined below. The fields for TM polarization are given by

$$E_{\perp,j}(x,q) = \left[E_j^+(x,q) - E_j^-(x,q)\right]\frac{q}{n_j}, \tag{4b}$$

$$= t^+_{i'j(i'+1)}\left[e^{iqx} - r_{j(i'+1)}e^{iq(2d_j-x)}\right]\frac{q}{n_j}, \tag{4c}$$

and

$$E_{\parallel,j}(x,q) = \left[E_j^+(x,q) + E_j^-(x,q)\right]\sqrt{1-\left(\frac{q}{n_j}\right)^2}, \tag{4d}$$

$$= t^+_{i'j(i'+1)}\left[e^{iqx} + r_{j(i'+1)}e^{iq(2d_j-x)}\right]\sqrt{1-\left(\frac{q}{n_j}\right)^2}, \tag{4e}$$

and for polarization TE

$$E_{\perp,j}(x,q) = 0, \tag{4f}$$

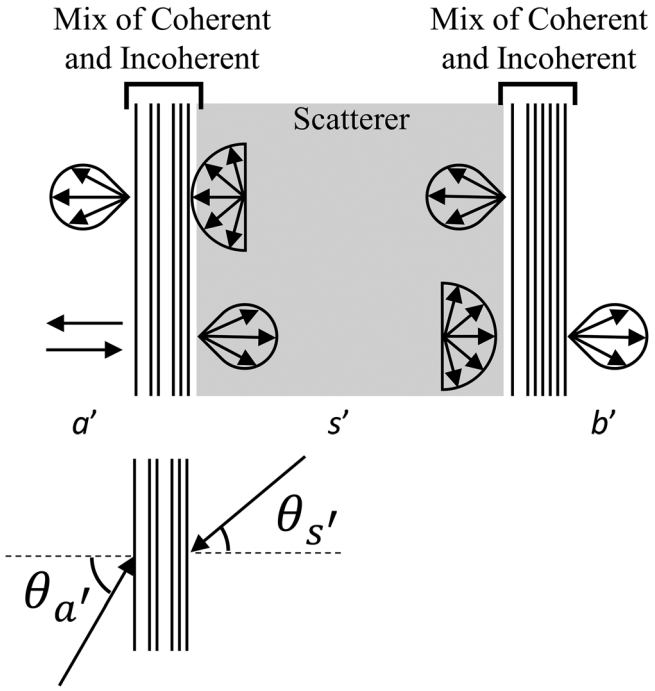

FIG. 1. Structure considered in this work, a scattering layer surrounded by arbitrary combinations of coherent and incoherent layers. Incoherent layers are enumerated a' to b'. The scattering layer is denoted as the s'th layer. Light that enters the scattering layer is fully randomized before returning to either interface of this layer.

$$E_{\|,j}(x,q) = t^{+}_{i'j\,(i'+1)}[e^{iqx} + r_{j\,(i'+1)}e^{iq(2d_j-x)}], \tag{4g}$$

where

$$t^{+}_{i'j\,(i'+1)} = \frac{t_{i'j}}{1 - r_{j\,i'}r_{j\,(i'+1)}e^{i2qd_j}}, \tag{4h}$$

(with assumed polarization and q dependence of Fresnel equations). As shown in Fig. 2, E is the normalized electric field with $\|$ or $\perp$ denoting the components of the field either perpendicular or parallel to the surface, and $+$ and $-$ superscripts refer to the forward and backward travelling waves, respectively; α_j is the absorption coefficient of the j^{th} layer; d_j is the thickness of the j^{th} layer; $r_{j\,(i'+1)}$ is the reflection coefficient from the rear of the jth layer through all the layers up to the $(i'+1)^{\text{th}}$ layer; $r_{j\,i'}$ is the reflection coefficient from the j^{th} layer to the i'^{th} layer; and $t_{i'j}$ is the transmission coefficient from the i'^{th} layer to the j^{th} layer.

For a non-scattering structure containing both coherent and incoherent layers, the total absorption in a coherent layer j can be calculated by considering how many times the light passes through the coherent layer stack containing the j^{th} coherent layer and with what intensity. Here, as depicted in Figs. 2 and 3, we denote the last incoherent layer before the coherent layer stack (containing j) as the i'^{th} layer and the first incoherent layer after the stack as the $(i'+1)^{\text{th}}$ layer. When no scattering is present, the absorption in layer j due to light originating in an incoherent layer, a', and traveling to an incoherent layer, b', is given by

$$A_{a'j\,b'}(q) = \frac{\mathcal{A}_{i'j\,b'}(q)T_{a'\,i'}(1-A_{i'})}{1 - R_{i'\,a'}R_{i'\,b'}(1-A_{i'})^2}, \tag{5a}$$

where

$$\mathcal{A}_{i'jb'}(q) = \tilde{A}_{i'\,j\,(i'+1)}(q) + \frac{\tilde{A}_{(i'+1)ji'}(q)T_{i'\,(i'+1)}R_{(i'+1)\,b'}\left(1-A_{(i'+1)}\right)^2}{1-R_{(i'+1)\,i'}R_{(i'+1)\,b'}\left(1-A_{(i'+1)}\right)^2}, \tag{5b}$$

and $A_{i'}$ and $A_{(i'+1)}$ are the absorption for a single pass through the i'^{th} or $(i'+1)^{\text{th}}$ layer, respectively (defined in the usual way as $1 - |\exp(\mathrm{i}\,d\,k_0\sqrt{n^2-q^2})|^2$). Again, polarization and q dependence are assumed in all reflection and transmission coefficients. Note that when the a'th layer is also the i'th layer, $T_{a'\,i'} = 1$, $R_{i'\,a'} = 0$, and $A_{i'} = 0$. Similarly, when the $(i'+1)$th layer is also the b'th layer, $R_{(i'+1)\,b'} = 0$ and $A_{(i'+1)} = 0$. Absorption in an incoherent layer is given by similar equations. For example, the absorption in an arbitrary incoherent layer i' due to light originating in the a'^{th} layer and ending in the b'th layer is given by

$$\mathrm{A}_{a'i'b'}(q) = \left[1 + (1-A_{i'})R_{i'\,b'}\right]\frac{T_{a'\,i'}A_{i'}}{1 - R_{i'\,a'}R_{i'\,b'}(1-A_{i'})^2}. \tag{5c}$$

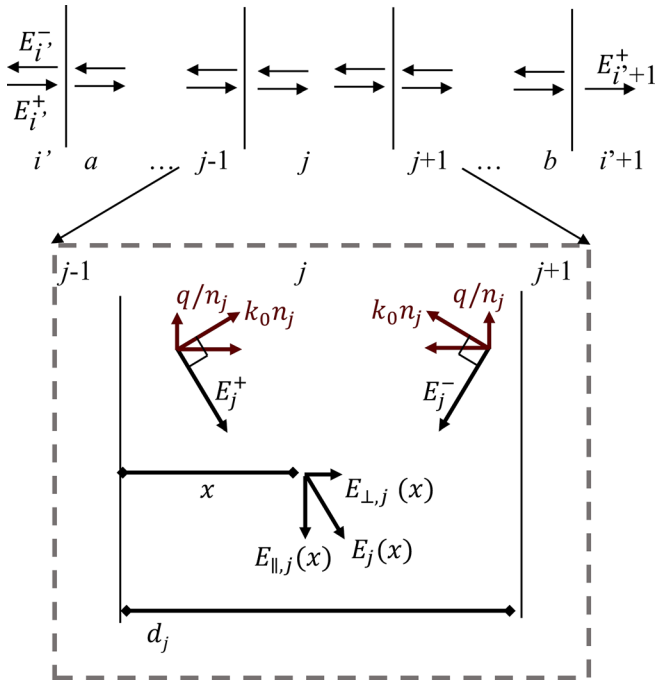

FIG. 2. Schema of the electric field components in each layer with numbering notation used to describe stacks of coherent layers. Coherent layers are enumerated a through b, with light originating and ending in semi-infinite spaces labeled i' and $i'+1$. In general, j will be used to denote the coherent layer of interest. The arrows between the layers represent the direction of forward and backward traveling waves. Zoom-in on layer j shows the naming conventions for the fields and k-vectors. The total field consists of forward and backward travelling waves denoted with plus and minus superscripts, respectively. The total field can be decomposed into parallel and perpendicular components (marked by $\|$ and $\perp$ subscripts, respectively). x is the distance from the light incidence side (i.e., $\boldsymbol{x} = \mathbf{0}$ at the boundary of layers j-1 and j in this figure).

Finally, we are able to calculate our main result, the absorption in any layer of a planar structure in the presence of a scattering layer. The absorption in the $\mathbb{z}^{\text{th}}$ layer (here z is used as a dummy variable representing any layer, coherent or otherwise) due to light impinging on the front (a'^{th} layer) of our scattering structure with scattering occurring in the s'^{th} layer can be calculated. When layer $\mathbb{z}$ is before the scattering layer, the absorption in layer $\mathbb{z}$ is

$$A^{\text{tot}}_{a'\,\mathbb{z}\,b'} = \langle A_{s'\,\mathbb{z}\,a'}(q)\rangle + \frac{\langle T_{a'\,s'}\rangle\langle A_{\text{diff},\ s'\mathbb{z}\,a'}\rangle\langle R_{\text{scat}}\rangle}{1-\langle R_{\text{diff},\,s'a'}\rangle\langle R_{\text{scat}}\rangle}, \tag{6a}$$

where

$$\langle R_{\text{scat}}\rangle = (1-\tau_{\text{int}})\rho_{\text{int}} + \frac{(\tau_{\text{int}}\rho_{\text{int}})^2\langle R_{\text{diff},s'b'}\rangle}{1-(1-\tau_{\text{int}})\rho_{\text{int}}\langle R_{\text{diff},s'\,b'}\rangle}, \tag{6b}$$

and when layer $\mathbb{z}$ is after the scattering layer, the absorption in this layer is

$$A^{\text{tot}}_{a'\mathbb{z}\,b'} = \frac{\langle A_{\text{diff},s'\,\mathbb{z}\,b'}\rangle\langle T_{\text{scat}}\rangle}{1-\langle R_{\text{diff},s'b'}\rangle\langle R_{\text{scat}}\rangle}, \tag{6c}$$

where

$$\langle R_{\text{scat}}\rangle = (1-\tau_{\text{int}})\rho_{\text{int}} + \frac{(\tau_{\text{int}}\rho_{\text{int}})^2\langle R_{\text{diff},s'a'}\rangle}{1-(1-\tau_{\text{int}})\rho_{\text{int}}\langle R_{\text{diff},s'a'}\rangle}, \tag{6d}$$

and

$$\langle T_{\text{scat}}\rangle = \frac{\tau_{\text{int}}\rho_{\text{int}}\langle T_{a's'}\rangle}{1-(1-\tau_{\text{int}})\rho_{\text{int}}\langle R_{\text{diff},s'a'}\rangle}, \tag{6e}$$

where $A_{\text{diff},\,s'\mathbb{z}\,a'}$ is defined as

$$A_{\text{diff},\,s'\mathbb{z}\,a'} = 2\int_0^{\frac{\pi}{2}} \text{A}_{s'\mathbb{z}\,a'}(n_{s'}\sin(\theta_{s'}))\cos(\theta_{s'})\sin(\theta_{s'})d\theta_{s'} \tag{6f}$$

with a similar expression for $A_{\text{diff},\,s'\mathbb{z}\,b'}$.

In the calculations above, we have made a few important assumptions. We summarize these assumptions here for clarity. First, we assume, that light passing through the scattering layer becomes completely randomized, so that the scattering does not depend on incident angle (beyond Fresnel coefficients for transmission/reflection into and out of the scattering layer). This condition is required to create analytic algebraic expressions and is met for many scattering structures. If the light is not fully randomized, other methods are required, e.g., a Monte Carlo approach.[6,25] Second, we assumed that the scatterer is weakly absorbing. This condition is required to define random scattering in the usual way as producing equal power per solid angle. When this condition is not met, random can only be properly defined as filling all optical modes. In Appendix A we also consider the use of strongly absorbing scatterers where the scatterers are well separated from the next material interface. Third, we assumed that the interfaces are planar and parallel to a good approximation. Large deviations from this approximation result in additional scattering. However, small deviations from planar and parallel are permitted (in fact, this deviation is one of the sources of incoherence in thick layers). In Appendix A, we also consider rough surfaces (which act as a type of scatterer) but under some simplifying assumptions that allow all calculations to be performed as if the structure contained only planar surface.

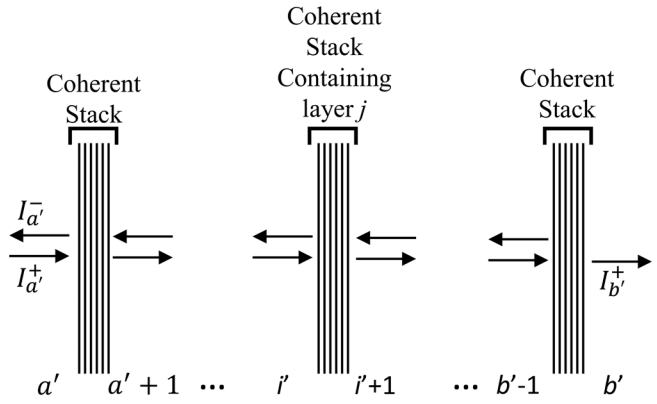

FIG. 3. Numbering scheme for a generic stack of coherent and in coherent layers. This structure has b′-1 incoherent layers between two semi-infinite layers all enumerated as layers a′ to b′. Between the incoherent layers are a total of b coherent layers (numbered 1 to b). The stack of coherent layers containing the jth coherent layer is immediately proceeded by the i′$^{\text{th}}$ incoherent layer. In direct analogy to Fig. 2, the arrows represent exchange of intensity between the layers. Note that this figure is in no way meant to denote any specific structure or layer ordering.

IV. SPECIAL CASES

When scattering structures are discussed there are several special cases that are typically examined which involve ideal layers and interfaces. Table I shows how various ideal front and back scatterers can be modeled. The first column lists the ideal condition under consideration, the second gives details of this idealization, and the third column gives a schematic view of that situation. The penultimate column describes how to set the parameters of the model to create that aspect, and the final column notes limitations of the described modeling. In this section we consider, ideal front and back scattering layers with additional special cases of potential interest described in Appendix A.

An ideal back reflector implies that the back reflector is perfectly reflective and/or the back reflector is perfectly scattering (Lambertian). Perfect reflectivity is achieved when there is no transmission ($\rho_{\text{int}}\tau_{\text{int}} = 0$) and no loss within the scatterer ($\rho_{\text{int}} = 1$). Perfect scattering is typically defined as producing a Lambertian intensity distribution

$$I(\theta) = I_0\cos(\theta), \quad \text{for } \theta \le \frac{\pi}{2}. \tag{7}$$

In the presence of resonant structures (coherent films) and absorption, this Lambertian scattering becomes poorly defined; however, the effect can be approximated by taking the scattering layer to have the same refractive index as the layer into which it is scattering (having index n)

$$P(n_{\text{eff}}) = \begin{cases} 1 & for\ \ n_{\text{eff}} = Re\{n\} \\ 0 & else. \end{cases} \tag{8}$$

TABLE I. Absorption modelling of special cases.

Conditions	Details	Schema	Parameter settings	Limitations/comments
Ideal back scatterer	Perfect (100%) reflection	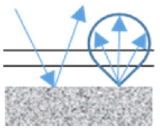	$\tau_{\text{int}} = 0$, $\rho_{\text{int}} = 1$	May still have specular reflection
	Perfect scatterer	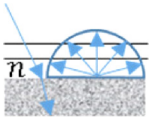	$P(n_{\text{eff}}) = \begin{cases} 1 & \text{for } n_{\text{eff}} = \text{Re}\{n\} \\ 0 & else \end{cases}$	May not be Lambertian in other layers. Large Im$\{n\}$ will cause deviation from Lambertian
Ideal intermediate or top scatterer	Perfect scattering into first layer above scatterer	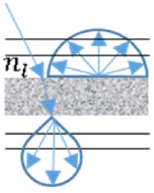	$P(n_{\text{eff}}) = \begin{cases} 1 & \text{for } n_{\text{eff}} = \text{Re}\{n_l\} \\ 0 & else \end{cases}$	May not be Lambertian in other layers. Large Im$\{n_l\}$ will cause deviation from Lambertian
	Perfect scattering into first layer after scatterer	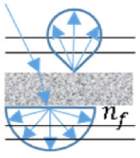	$P(n_{\text{eff}}) = \begin{cases} 1 & \text{for } n_{\text{eff}} = \text{Re}\{n_f\} \\ 0 & else \end{cases}$	See above.
	Perfect scattering both directions	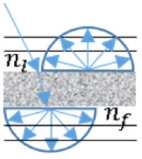	When calculating $R_{a's'}$ $R_{\text{diff},s'a'}$, and $A_{\text{diff},s'\mathbb{z}a'}$: $P(n_{\text{eff}}) = \begin{cases} 1 & \text{for } n_{\text{eff}} = \text{Re}\{n_l\} \\ 0 & else \end{cases}$ When calculating $R_{\text{diff},s'b'}$, $A_{\text{diff},s'\mathbb{z}b'}$: $P(n_{\text{eff}}) = \begin{cases} 1 & \text{for } n_{\text{eff}} = \text{Re}\{n_f\} \\ 0 & else \end{cases}$	See above.
	Perfect antireflection	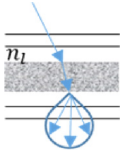	$P(n_{\text{eff}}) = \begin{cases} 1 & \text{for } n_{\text{eff}} = \text{Re}\{n_l\} \\ 0 & else \end{cases}$ $\tau_{\text{int}} = 1$, $\rho_{\text{int}} = 1$	Light leaving front after reflections from deeper layers will have Lambertian scattering.

The real part is taken here to maintain our assumption of negligible absorption in the scattering layer. Note that when Im$\{n\}$ becomes large, the reflection at an interface between two materials with different indices, Re$\{n\}$ and n, respectively, becomes non-zero and is no longer angle independent. In that case, Eq. (8) results in a poor approximation. For example, GaAs has an index of $n = 2.72 + 4.26\text{i}$ at a wavelength of 250 nm (near an absorption resonance),[26] which would produce a 38% TE reflection at a Re$\{n\}/n$ interface for normal incidence and 41% for 90° incidence. However, at a wavelength of 550 nm, GaAs has an index of $n = 4.06 + 0.27\text{i}$,[26] which would produce a 0.11% reflection at a Re$\{n\}/n$ interface for normal incidence and 0.12% for 90° incidence.

This same process can be used to model ideal intermediate or top scatterers. To produce Lambertian scattering from any given interface into a medium with index, n, the scatterer must have an effective index given by Re$\{n\}$. Note that because we describe the internal structure of the scattering layer with only phenomenological constants τ_{int} and ρ_{int}, there is no requirement that the effective index of the scattering at the front and the back sides of the scattering layer be the same. Physically, this may correspond to an index grading from one side to the other or scatterers placed at an interface between dissimilar materials (this case is explored further in Appendix A). As an example, to produce Lambertian scattering at both sides of the scattering layer, we have the following.

For $R_{\text{diff},s'a'}$, $R_{a's'}$, and $A_{\text{diff},s'\mathbb{z}\,a'}$

$$P(n_{\text{eff}}) = \begin{cases} 1 & for \;\; n_{\text{eff}} = Re\{n_l\} \\ 0 & else, \end{cases} \tag{9a}$$

and for $R_{\text{diff},\,s'b'}$, $A_{\text{diff},s'z\,b'}$

$$P(n_{\text{eff}}) = \begin{cases} 1 & for \;\; n_{\text{eff}} = Re\{n_f\} \\ 0 & else, \end{cases} \tag{9b}$$

where n_l is the index of the last layer before the scattering layer, n_f is the index of the first layer after the scattering layer and $\mathbb{z}$ is the layer (coherent or incoherent) where the absorption is to be calculated.

Lastly, we consider an ideal antireflection coating on the top scatterer. This situation can be modeled by setting the top

interface of the scatterer to be a perfect scatterer, but without allowing any reflection or absorption as light passes through the scattering layer (setting $\tau_{int} = 1$ and $\rho_{int} = 1$). Note that the top perfect scattering requirement prevents reflection from this surface at all incident angles and all wavelengths (as long as $\mathrm{Im}\{n_l\}$ is small, per the above discussion).

Other special cases are outlined in Appendix A, including absorbing scatterers and textured surfaces.

V. NUMERICAL DEMONSTRATIONS

Figure 4 shows four examples of multilayer structures with scattering layers interspersed to illustrate some of the potentially useful designs that can be calculated using the above-outlined method. For a thin-film photovoltaic device, it is desirable to place a scattering object either on the top surface, the back surface, or in the middle of the device to increase the optical path length.[27–29] However, it is not always obvious where the most appropriate placement should be *a priori*. Figures 4(a)–4(c) shows three examples of a thin a-Si layer with a scattering layer placed at different positions within the structure. The layer stack consists of two coherent layers, a 70 nm SiN layer (often used as an anti-reflection coating or a spacer layer between the scatterer and the active material) and a 30 nm absorptive a-Si layer, and a scattering layer. The scattering layer is characterized by $\tau_{int} = 0.95$ and $\rho_{int} = 0.95$ (similar to experimental values below), and a scattering probability of $P(n_{eff} = 1.5) = 1$ is used to represent a simplified scattering case from a material with an index similar to glass (note that a single effective index is considered here for clarity but an ensemble of indices should generally be used for more precise, real world applications, see for example, Ref. 19). In addition to the wavelength-dependent absorption, the predicted short-circuit current for an ideal solar cell can be calculated. Taking the a-Si as the photovoltaic layer, and assuming that each absorbed photon generates an electron-hole pair that is subsequently collected, the short-circuit current density is

$$J_{sc} = e\int_0^{\infty} S(\lambda) * A^{\mathrm{tot}}_{a'\,\mathbb{z}\,b'}(\lambda) * \left(\frac{\lambda}{hc}\right) d\lambda, \tag{10}$$

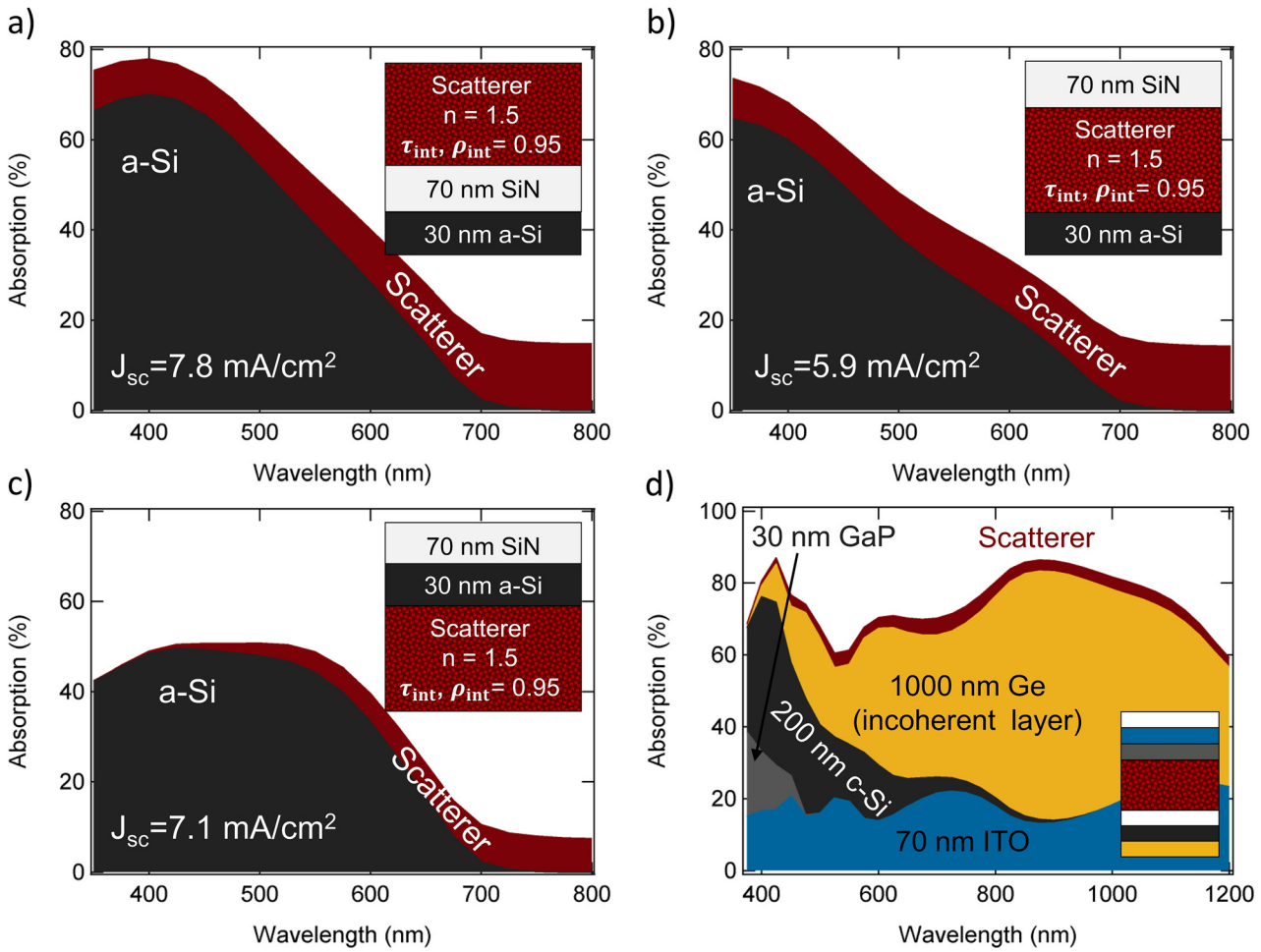

FIG. 4. Examples of absorption calculated in individual layers using the method described above. (a)–(c) Plots show the separately determined absorption in an a-Si layer and a scattering layer when the scattering layer is (a) on the top, (b) in the middle, or (c) on the bottom of the multilayer stack. In all cases, the structure contains a SiN thin-film above the a-Si layer, and the scatterer has an effective refractive index of 1.5 and an internal absorptivity and transmissivity of 5% and 95%, respectively. Each plot is also labeled with a predicted short-circuit current density corresponding to an ideal device under AM 1.5G illumination. This value could not have been accurately calculated without first determining the absorption in each layer. (d) Shows the absorption in each layer of a more complicated multilayer structure. The layers are color coded by material and placement within the stack (see inset). The white layers are 100 nm of SiO_2 on the top and 80 nm of SiN in the lower half. The scattering layer has the same parameters as used in (a)–(c). Note that in all cases the absorption of the scatterer is calculated as the difference between the total absorption and that of all other structures. Illumination is from the top.

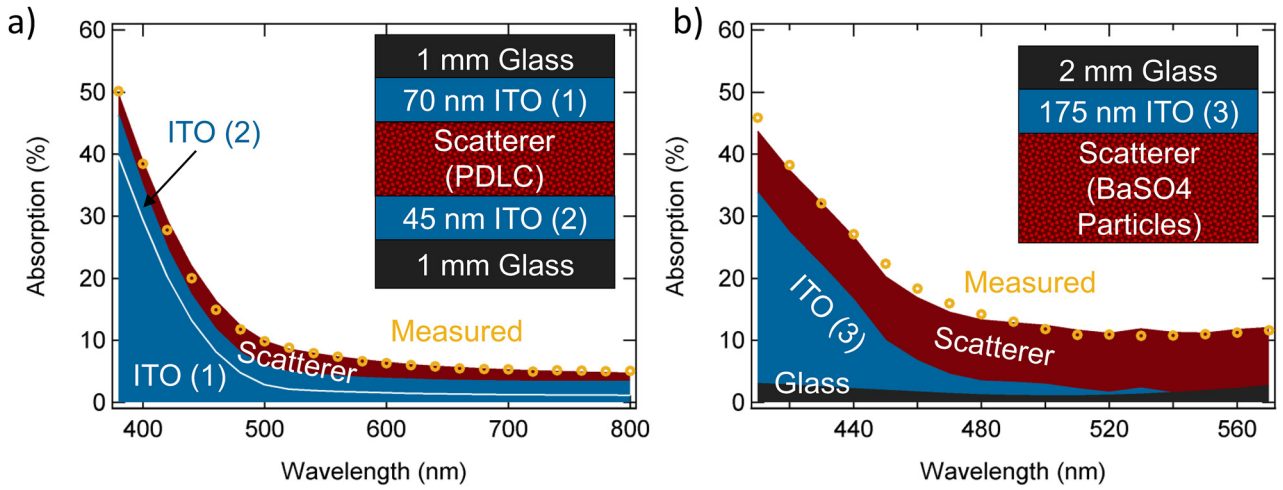

FIG. 5. Experimentally determined total absorption (open circles) agrees with the total absorption calculated from our model by adding up the absorption in the individual layers. The model enables the determination of how much light was absorbed in each layer, which was not possible through the absorption measurement alone. (a) A scattering structure containing two (different) absorbing ITO layers and a scattering layer composed of a polymer dispersed liquid crystal (PDLC) suspension. Note that the absorptivity of the glass used in this device is found to be immeasurably small and is not shown here. (b) Absorption in a scattering structure composed of barium sulfate nanoparticles applied to an ITO coated glass slide.

where λ is the incident wavelength, $S(\lambda)$ is the spectral power density (taken to be AM1.5G illumination) and e, h, and c are electron charge, Planck's constant and the speed of light, respectively. Note that this calculation can only accurately be performed when the per-layer absorption ($A^{\text{tot}}_{a'\mathbb{z}b'}(\lambda)$) is known. Using the above equations, we are able to accurately determine that, for these structures (Figs. 4(a)–4(c)), the scattering layer should be placed on the top for best performance, i.e., maximized absorption in the a-Si layer.

Figure 4(d) shows the absorption within each layer of a structure with a large number of absorbing layers. The colors in the shaded regions correspond to the layers shown in the inset of this figure. This structure uses the same scattering layer parameters used in Figs. 4(a)–4(c) and has two non-absorbing layers (depicted as white in the inset): a 100 nm SiO_2 layer on the top and an 80 nm SiN layer in the lower half. The bottom bulk Ge layer (yellow) is an incoherent layer. This structure is meant to roughly correspond to a more complex device where absorption can occur in specific, isolated layers (e.g., a multi-junction solar cell) where a scattering layer has been placed between the two absorbing layers (note: this is not meant to be a suggestion of an actual device; the materials were chosen to give an example of the method only). Again, this method allows for accurate determination of absorption in each layer individually.

In addition to the computational examples provided above, two experiments are conducted and our method is used to show how the absorption in each of the individual layers may be determined in a real world scenario. In both examples, the scattering characteristics are determined experimentally using a custom gonioreflectometer, as described in Ref. 19. The values of τ_{int} and ρ_{int} are fit for each of the scattering layers using transmission and absorption measurements on independent structures. The indices and thicknesses of the layers are determined using ellipsometry and confirmed by step height measurements from an atomic force microscope. Absorption and transmissions measurements are performed using the integrating sphere setup described in our previous work.[19]

Figure 5(a) shows the measured total absorption (circles) for a structure consisting of two layers of ITO (indium tin oxide) on glass separated by a scattering layer (a polymer dispersed liquid crystal (PDLC[30])) and the calculated absorption in each of the individual layers. Similarly, Fig. 5(b) shows the measured and calculated absorption for an ITO coated glass slide with a scattering layer on the back (barium sulfate nanoparticle paint).[19] In both cases, the total calculated absorption closely matches the measured total absorption. These simple examples are presented merely to demonstrate the experimental utility of the theoretical framework outlined above and its applicability to a variety of samples.

VI. CONCLUSIONS

Here we presented an analytical description of absorption in individual layers of stratified medium containing a scattering layer that randomizes the light. We showed how this calculation can be carried out in the presence of an arbitrary set of layers containing both coherent and incoherent layers. We considered some important special cases. Finally, we offered several theoretical and experimental examples to demonstrate some of the potential applications of this approach. The generality of these equations should be of particular interest with perhaps the most severe restriction being internal randomization of light within the scattering layer. However, with this criterion met, the theory requires only that the scattering layers be described by two experimentally measurable parameters.[19] Thus, the equations presented here are completely agnostic toward the actual nature of the scatterer and enable the calculation of absorption within each layer individually, which should aid in the development and screening of many potential optoelectronic devices designs, e.g., thin-film photovoltaics, photodetectors, and so on.

ACKNOWLEDGMENTS

Authors acknowledge the University of Maryland and its Fab Lab, as well as M. S. Leite for helpful comments and suggestions.

APPENDIX

The following tables are provided as a reference guide to several additional cases of particular interest and as a summary of the variables used here.

APPENDIX A: TABLE OF ADDITIONAL SPECIAL CASES

Conditions	Details	Schema	Parameter settings	Limitations/comments
Embedded scatterers including strongly absorbing particles	In non-absorbing layer	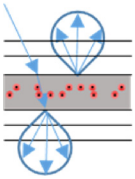	Treat embedding layer as the scattering layer $P(n_{\text{eff}}) = \begin{cases} 1 & \text{for } n_{\text{eff}} = n_{\min} \\ 0 & else \end{cases}$ where $n_{\min}$ is smaller $Re\{n\}$ of either the particles or embedding material	The physical situation described is only accurately modeled if the strongly absorbing particles are far from interfaces
Scatterers at interface including strongly absorbing particles	In non-absorbing layers	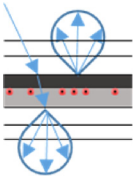	Treat two surrounding layers as a single scattering layerUpper half: $P(n_{\text{eff}}) = \begin{cases} 1 & \text{for } n_{\text{eff}} = n_{\min} \\ 0 & else \end{cases}$ where n_{min} is smaller $Re\{n\}$ of the particles or upper material. Lower half: $P(n_{\text{eff}}) = \begin{cases} 1 & \text{for } n_{\text{eff}} = n_{\min} \\ 0 & else \end{cases}$ where $n_{\min}$ is smaller $Re\{n\}$ of the particles or lower material.	The physical situation described is only accurately modeled if the strongly absorbing particles are far from interfaces
Texturing	Perfectly random surface on top	Actual:  Modeled: 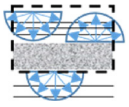	Model with diffuse illumination: Change $\langle T_{a's'} \rangle$ and $\langle R_{a's'} \rangle$ to $\langle T_{\text{diff},a's'} \rangle$ and $\langle R_{\text{diff},a's'} \rangle$ And model with a scattering layer just below last textured surface with: $P(n_{\text{eff}}) = \begin{cases} 1 & \text{for } n_{\text{eff}} = \text{Re}\{n_f\} \\ 0 & else \end{cases}$ And $\tau_{\text{int}} = 1$, and $\rho_{\text{int}} = 1$	Ignores multiple reflections at textured surface
	Perfectly random back reflector	Actual: 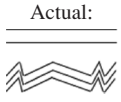 Modeled: 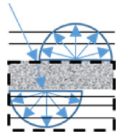	Model with scattering layer inserted in last layer before textured layers. Set scattering layer as "Perfect scattering both directions" from Table I.	Ignores multiple reflections at textured surface

APPENDIX B: TABLE OF VARIABLES FOR ABSORPTION MODELLING

Variable	Description	Equations
I	Scattered intensity per solid angle	(1)
I_0	Arbitrary normalization constant	(1)
θ	Angle between surface normal and propagation direction	(1)
T	Transmitted intensity	(1)
n_{eff}	Effective index of scattering layer	(1)
n	Index of a non-scattering layer	(1)
$P(n_{\text{eff}})$	Probability of scattering from a given effective index	(1)
$R_{a'b'}$	Reflected intensity of light travelling from the a'^{th} to b'^{th} incoherent layer	(2a), (2c), (3a), (3b), (5a)–(5c)
$T_{a'b'}$	Transmitted intensity of light travelling from the a'^{th} to b'^{th} incoherent layer	(2a)–(2c), (5a)–(5c)
$A_{a'b'}$	Total absorption for light travelling from the a'^{th} to b'^{th} incoherent layer	(2c)
$R_{\text{diff},s'a'}$	Total integrated diffuse reflection for light traveling from the scatterer to incoherent layer a'	(2a), (2b), (2d), (3a), (3b), (6a)–(6e)

(*Continued*.)

Variable	Description	Equations
$T_{\text{diff},s'a'}$	Total integrated diffuse transmission for light traveling from the scatterer to incoherent layer a'	(2a), (2e)
R_{scat}	Total reflection for light starting just inside the scattering layer and propagating to the back half-space.	(2a), (2b), (2d), (6a)–(6d)
T_{scat}	Total transmission for light starting just inside the scattering layer and propagating to the back half-space.	(2a), (2b), (2e), (6c), (6e)
τ_{int}	Ratio of the transmitted intensity to ρ_{int} from the scatterer	(2d), (2e), (6b), (6d), (6e)
ρ_{int}	Sum of the reflected light and transmitted light intensities from the scatterer	(2d), (2e), (6b), (6d), (6e)
$\theta_{s'}$	Angle between surface normal and propagation direction inside scattering material for a given n_{eff}	(3a), (6f)
q	Relative parallel component of k-vector	(4a)–(4h), (5a)–(5c), (6a)
$k_{\parallel}$	Parallel component of k-vector	Inline only
k_0	Magnitude of k-vector in free-space	Inline only
$\tilde{A}_{ajb}$	The absorption in the jth layer for light passing through the coherent stack starting from layer a and going to layer m	(4a), (5b)
c	Speed of light in vacuum	(4a)
ε_0	Permittivity of free-space	(4a)
α_j	Absorption coefficient in j^{th} layer	(4a)
n_j	Refractive index in j^{th} layer	(4a)–(4e)
$E_{\perp,j}$	Perpendicular component of electric field in j^{th} layer	(4b), (4c), (4f)
$E_{\parallel,j}$	Perpendicular component of electric field in j^{th} layer	(4d), (4e), (4g)
x	Distance from front of j^{th} layer	(4a)–(4e), (4g)
d_j	Thickness of j^{th} layer	(4c), (4e), (4g), (4h)
$r_{ja'}$	Field reflection coefficient for all layers from layer j to the next incoherent layer a'	(4c), (4e), (4g), (4h)
$t_{ja'}$	Field transmission coefficient for all layers from layer j to the next incoherent layer a'	(4h)
$t^{+}_{a'jb'}$	Total field transmission coefficient from the a'^{th} layer to the j^{th} layer, including cavity field enhancement due to layers j through b'.	(4c), (4e), (4g), (4h)
$A_{a'jb'}$	The absorption, in the j^{th} layer (thin film) between any two incoherent layers, a' and b', with light originating in the a'^{th} layer and ending in the b'^{th} layer	(5a), (6a), (4f)
$\mathcal{A}_{a'jb'}(q)$	Absorption in j^{th} layer (thin film) between two incoherent layers a' and b' where the a'^{th} layer is the last incoherent layer before layer j	(5a), (5b)
$A_{a'}$	Absorption for a single pass through the a'^{th} (incoherent) layer	(5a)–(5c)
$A^{\text{tot}}_{s'\,\mathbb{Z}\,a'}$	Absorption in $\mathbb{Z}^{\text{th}}$ layer for light leaving scattering layer s' and ending in incoherent layer a'	(6a), (6c), (6f), (9a), (9b)
J_{sc}	Short circuit current density	(10)
λ	Wavelength of light in free-space	(10)
$S_{AM1.5G}(\lambda)$	Spectral power density for AM1.5G illumination	(10)
h	Plank's constant	(10)

[1]L. A. A. Pettersson, L. S. Roman, and O. Inganäs, J. Appl. Phys. **86**, 487 (1999).
[2]E. Centurioni, Appl. Opt. **44**, 7532 (2005).
[3]V. Liu and S. Fan, Comput. Phys. Commun. **183**, 2233 (2012).
[4]A. Lin, S. M. Fu, Y. K. Zhong, C. W. Tseng, P. Y. Chen, and N. P. Ju, J. Appl. Phys. **115**, 153105 (2014).
[5]J. Grandidier, D. M. Callahan, J. N. Munday, and H. A. Atwater, Adv. Mater. **23**, 1272 (2011).
[6]A. Abass, C. Trompoukis, S. Leyre, M. Burgelman, and B. Maes, J. Appl. Phys. **114**, 33101 (2013).
[7]N. Tucher, J. Eisenlohr, P. Kiefel, O. Höhn, H. Hauser, M. Peters, C. Müller, J. C. Goldschmidt, and B. Bläsi, Opt. Express **23**, A1720 (2015).
[8]J. Eisenlohr, N. Tucher, O. Höhn, H. Hauser, M. Peters, P. Kiefel, J. C. Goldschmidt, and B. Bläsi, Opt. Express **23**, A502 (2015).
[9]J. D. Joannopoulos, S. G. Johnson, J. N. Winn, and R. D. Meade, *Photonic Crystals: Molding the Flow of Light*, 2nd Ed. (Princeton University Press, 2011).
[10]Z. Yu, A. Raman, and S. Fan, Proc. Natl. Acad. Sci. U.S.A. **107**, 17491–17496 (2010).
[11]P. Nitz, J. Ferber, R. Stangl, H. Rose Wilson, and V. Wittwer, Sol. Energy Mater. Sol. Cells **54**, 297 (1998).
[12]D. M. Callahan, J. N. Munday, and H. A. Atwater, Nano Lett. **12**, 214 (2012).
[13]E. Yablonovitch, J. Opt. Soc. Am. **72**, 899 (1982).
[14]H. R. Stuart and D. G. Hall, J. Opt. Soc. Am. A **14**, 3001 (1997).
[15]E. A. Schiff, J. Appl. Phys. **110**, 104501 (2011).
[16]J. N. Munday, D. M. Callahan, and H. A. Atwater, Appl. Phys. Lett. **100**, 121121 (2012).
[17]K. R. Catchpole, S. Mokkapati, and F. J. Beck, J. Appl. Phys. **109**, 84519 (2011).
[18]J. Murray and J. N. Munday, J. Appl. Phys. **119**, 23104 (2016).
[19]C. C. Katsidis and D. I. Siapkas, Appl. Opt. **41**, 3978 (2002).
[20]C. L. Mitsas and D. I. Siapkas, Appl. Opt. **34**, 1678 (1995).
[21]B. Lipovšek, J. Krč, O. Isabella, M. Zeman, and M. Topič, J. Appl. Phys. **108**, 103115 (2010).
[22]W. E. Vargas and G. A. Niklasson, J. Opt. Soc. Am. A **14**, 2243 (1997).
[23]W. E. Vargas, P. Greenwood, J. E. Otterstedt, and G. A. Niklasson, Sol. Energy **68**, 553 (2000).
[24]J. E. Cotter, J. Appl. Phys. **84**, 618 (1998).
[25]U. Rau, U. W. Paetzold, and T. Kirchartz, Phys. Rev. B **90**, 35211 (2014).
[26]G. E. Jellison, Opt. Mater. **1**, 151 (1992).
[27]H. A. Atwater and A. Polman, Nat. Mater. **9**, 205 (2010).
[28]V. E. Ferry, J. N. Munday, and H. A. Atwater, Adv. Mater. **22**, 4794 (2010).
[29]M. L. Brongersma, Y. Cui, and S. Fan, Nat. Mater. **13**, 451 (2014).
[30]F. Bloisi, P. Terrecuso, L. Vicari, and F. Simoni, Mol. Cryst. Liq. Cryst. Sci. Technol. Sect. A **266**, 229 (1995).